



Combination of Sonochemical Synthesis and Calcination of Graphene-TiO₂ Nanocomposite for Efficient Photocatalytic Degradation of Methyl Orange Dye

S. LAXMI PRIYA¹, N. MANOJ², K. LEON PRASANTH³, E. NISSAM⁴, S. SUGUNAN⁵ and K.M. RAJESH^{1*}

¹P.G. and Research Department of Chemistry, Sree Narayana College, Nattika-680566, India

²P.G. and Research Department of Chemistry, Sanatana Dharma College, Sanatanapuram, Kalarcode-688003, India

³Post Graduate and Research Department of Chemistry, Zamorin's Guruvayurappan College, Calicut -673014, India

⁴P.G. and Research Department of Chemistry, MES Mampad College (Autonomous), Malappuram-676542, India

⁵Department of Applied Chemistry, Cochin University of Science and Technology, Cochin-682022, India

*Corresponding author: E-mail: rajeshkmamangalam@gmail.com

Received: 27 February 2024;

Accepted: 9 July 2024;

Published online: 25 July 2024;

AJC-21715

In this work, a nanostructured graphene-TiO₂ nanocomposite was prepared by modified sonochemical method followed by calcination process at 400 °C and characterized by X-ray diffraction, transmission electron microscopy, UV visible spectroscopy, IR spectroscopy and X-ray photoelectron spectroscopy. The photocatalytic activity of the prepared sample was evaluated by photocatalytic degradation of methyl orange dye. On analysis, visible light absorption was found to be increased for the nanocomposite rather than pure TiO₂. About 75% degradation efficiency was exhibited by the prepared GT2 composite under sunlight irradiation.

Keywords: Graphene-TiO₂ nanocomposite, Photocatalytic degradation, Sonochemical method, Methyl orange.

INTRODUCTION

It is essential to find effective methods for removing organic pollutants from the environment, especially from water [1-4]. Even-though many methods such as ion-exchange, coagulation, adsorption, *etc.* are available for removing contaminants, they all offers many limitations such as lower efficiency, high cost, large residue production that all limits their usage. Photocatalytic dye degradation receives greater attention due to its efficient degrading ability, environmental adaptability enabling the conversion of toxic dye compounds upon irradiation under day light to harmless ecofriendly products like water and carbon dioxide. The ease of availability, lower toxicity, enhanced stability and economical aspects of TiO₂ received greater attention of researchers as an efficient material for organic dyes pollutant removal [5,6]. The limitation of titania due to the recombination of produced electron hole pairs can be effectively overcome by using a combination of TiO₂ nanoparticles with metal oxides or by using carbon based materials [7,8].

Among the carbon based materials, graphene oxide receives greater importance in preparing unique photocatalytic materials

for its large specific surface area, good heat conductivity and large electron-hole separation efficiency [9-14]. Thus, the efficiency of TiO₂ can be enhanced by stabilizing them on graphene oxide [15-17]. It was also found out that a combination of titania with graphene could reduce the level of electron-hole recombination, can elevate adsorption capacity and extend light absorption into the visible region [18-25]. The increased surface area offered by graphene-titania nanocomposite compared to pure titania nanomaterial provides more active sites and it will enhance contaminant degradation.

Graphene acts as a photosensitizer, allowing better light absorption and efficient charge separation, which leads to the improvement in the degradation of pollutants. Graphene has excellent electrical conductivity, which can facilitate the transport of photo-generated electrons from the TiO₂ surface. This accelerates the reaction kinetics and reduces charge recombination, leading to improved catalytic efficiency. One specific example where the combination of TiO₂ and graphene brings advantages is in the field of hydrogen production through water splitting [26]. TiO₂ is a well-established photocatalyst for water splitting, but its efficiency is limited due to the narrow light absorption

range and fast charge recombination. By incorporating graphene into TiO₂, the catalyst can effectively absorb visible light, reducing charge recombination and enhancing the overall photocatalytic activity for hydrogen production [27-29]. These advantages enable the development of more efficient and sustainable catalytic systems for various applications.

Methyl orange (MO) is one of the regularly used dyes in the textile industries and has been demonstrated to be quite hazardous, causing eye damage and perhaps resulting in long-term ocular disease. MO dye degradation can be achieved by different methods such as electrochemical degradation, photocatalysis, electrocatalytic degradation, pulsed power technique, low temperature catalytic degradation, advanced oxidation process, *etc.* of which photocatalytic degradation is more advantageous. The colouration of water by MO dye reduces sunlight penetration and thereby affecting the water oxygen concentration [30]. While comparing with the other methods like hydrothermal, sol-gel, ion-exchange, vapour deposition towards the degradation of MO dye, the processes involved in the sonochemical method could minimize agglomeration, which results in the enhancement of the crystal growth with the uniform shape and size in a short time [31-37]. In this work, a calcined graphene-titania (GT2) nanocomposite was synthesized by sonochemical method followed by calcination. The efficiency of photocatalytic activity of the synthesized nanocomposite was assessed by measuring the degradation of methyl orange dye under UV-light.

EXPERIMENTAL

Characterization: The XRD patterns were recorded using Bruker AXS D8 advanced X-ray Diffractometer. The Diffuse Reflectance UV-Visible spectra of the samples were measured using a Varian, Cary 5000 UV-visible NIR spectrophotometer. The FTIR spectra were recorded in Thermo-Nicolet, Avatar 370 FTIR Spectrometer in the range of 4000-400 cm⁻¹. The transmission electron microscopy (TEM) images were recorded using Jeol JEM 2100 ultrahigh resolution analytical electron microscope. The X-ray photoelectron microscopy was done on ESCA+ Omicron Nanotechnology (Oxford Instrument, Germany). For the sonochemical method, Dakshin Probe Sonicator, India (Frequency 22 KHz, 200 W) was used

Synthesis of graphene oxide: In a beaker, conc. H₂SO₄ (360 mL) was added to 40 mL H₃PO₄ and stirred well followed by the addition of 3 g graphite powder (99.99%, Sigma-Aldrich), 18 g KMnO₄ (99%, Sigma-Aldrich) and stirred continuously for 24 h. The resulting solution was cooled to room temperature and then poured to 400 g ice along with 27 mL of 30% H₂O₂ (Sigma-Aldrich). The resulting precipitate was centrifuged, washed with HCl followed by water and finally filtered to obtain a brown coloured graphene oxide [38,39].

Synthesis of graphene-titania nanocomposite (GT2): To 0.1 g graphene oxide, 20 mL ethanol was added and sonicated for 15 min followed by the addition of 50 mL isopropyl alcohol (99%, Sigma-Aldrich) and 5 mL titanium isopropoxide (97%, Sigma-Aldrich) and then sonicated again for further 30 min. To the resultant mixture, 80 mL demineralized water was added dropwise to obtain a white coloured sol, which was then aged at room temperature for 20 h and dried in an oven at 100 °C

for 8 h. Now, 5 mL hydrazine hydrate (50-60%, Sigma-Aldrich) was added to the dried sample and stirred. The resulting GT2 sample was then washed with deionized water twice and dried at 100 °C for 20 h. It was then calcined at 400 °C in a muffle furnace for 1 h resulting in the formation of a black coloured GT2 powder. Pure titania (T2) was also prepared in the same way except using graphene oxide and hydrazine hydrate.

Photocatalytic studies: Photodegradation of methyl orange (MO) dye were conducted on sunny days between 11.00 am and 2.30 pm. In brief, a 10 mL of MO (10⁻³ M) was diluted to 100 mL. Then, 10 mL of this solution, 0.03 g photocatalyst was added, stirred for 5 min in dark and then stirred again in direct sunlight for 45 min. Absorbance of this solution was measured at 529 nm. Studies were further conducted using varying amount of 0.02, 0.03 and 0.04 g of photocatalyst and labeled as GT2_{0.02}, GT2_{0.03}, GT2_{0.04}, respectively. Percent of degradation was calculated using the following relation:

$$\text{Degradation efficiency (\%)} = \frac{C_0 - C}{C_0} \times 100$$

where C₀ and C are the concentrations of dye before and after irradiation.

RESULTS AND DISCUSSION

XRD studies: The XRD spectra illustrated in Fig. 1 showed the peaks at 2θ = 25.413° (101), 38.017° (004), 48.104° (200), 54.619° (105) and 62.962° (204) giving the clear evidence of anatase phase formation [40-43] in a calcined graphene-titania nanocomposite. Depending on the specific synthesis method, conditions and precursors used, there could be slight presence of other phases such as secondary titanium dioxide phases or additional carbon phases. This might be the reason for the appearance of a peak at 31.00°. The inclusion of graphene oxide in titania leads to an interaction between them during the hydrolysis stage, which causes the peak width to broaden [44]. For the prepared GT2 nanocomposite, the average grain size calculated was in the range of 7.9 nm.

FTIR studies: Fig. 2 shows FTIR spectra of pure titania and calcined GT2 nanocomposite. A broad band for titania at 3424 cm⁻¹ appears due to the surface adsorbed water confirmed the presence of hydroxyl groups on the titania surface. A vibration band at 1620 cm⁻¹ was observed for graphene sheets in the prepared calcined GT2 nanocomposite. The presence of graphene oxide layer over titania in the synthesized photocatalyst material is confirmed as a strong band at 700-450 cm⁻¹ due to the Ti-O-Ti vibration. A new peak at 1125 cm⁻¹ is seen in the nanomaterial, which band is attributed to the vibrations of Ti-O-C bands [45].

UV-visible studies: The UV-visible spectra of calcined GT2 nanocomposite and titania are shown in Fig. 3. Titania exhibited a peak near 300-400 nm, however, an increase in visible light absorbance was found for calcined GT2 nanocomposite in the range of 300-700 nm, which might be due to the presence of graphene oxide. The absorption peak of calcined GT2 nanocomposite was found to be occurs above 450 nm and there seems to be a slight decrease in the band gap. The reason is attributed due to the physical effects of the ultrasonic irradiation results into improved micromixing and rapid

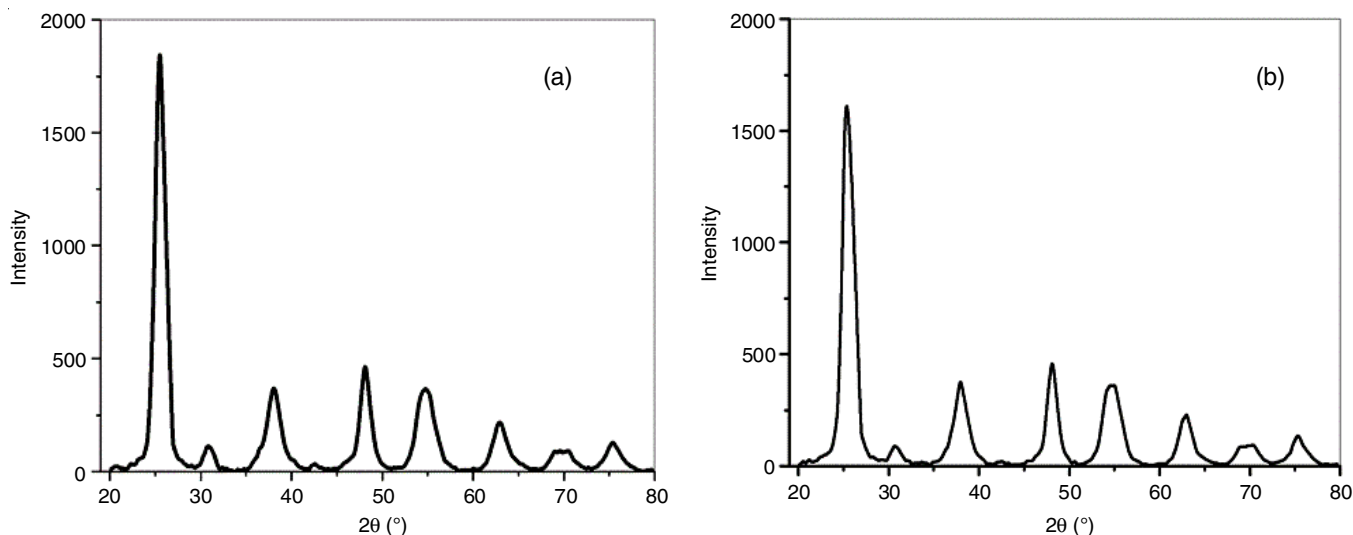


Fig. 1. XRD spectra of (a) graphene-titania nanocomposite (GT2) and (b) titania (T2)

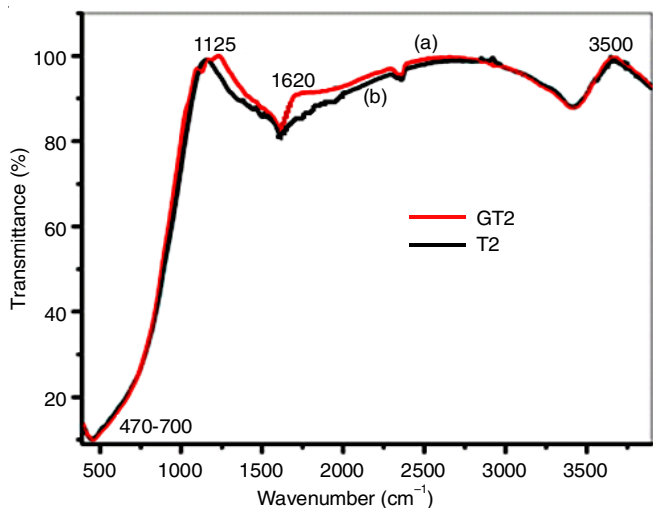


Fig. 2. FTIR spectra of (a) graphene-titania nanocomposite (GT2) and (b) titania (T2)

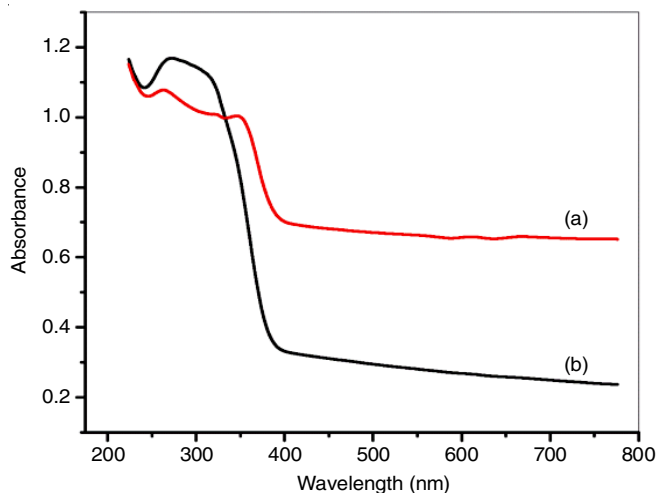


Fig. 3. UV-visible spectra of (a) graphene-titania nanocomposite (GT2) and (b) titania (T2)

nucleation leads to faster reaction to produce graphene-TiO₂ nanocomposite [46,47].

Morphological studies: The TEM and HRTEM images of calcined GT2 nanocomposite are depicted in Fig. 4, which revealed the graphene oxide-TiO₂ nanocomposite are decorated with high ordered morphology. The crystalline nature and anatase phase of the calcined GT2 nanocomposite were also confirmed from the HRTEM and SAED images. The reason is explained as the ultrasound induces a gradual rise in the

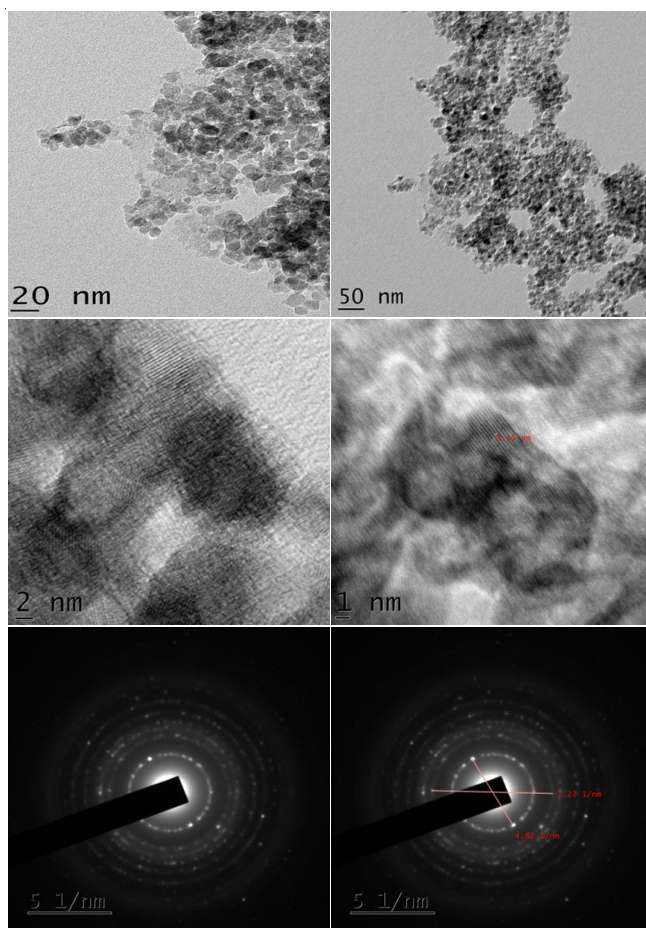


Fig. 4. TEM, HRTEM and SAED images of graphene-titania nanocomposite

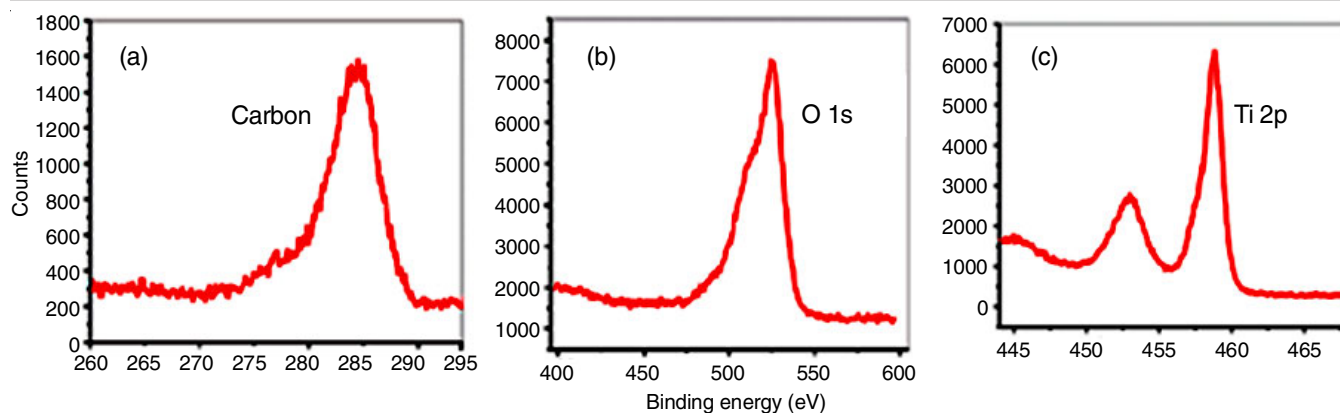


Fig. 5. XPS spectra of graphene-titania nanocomposite (GT2)

rate at which energy is dissipated, leading to the formation of a distinct and well-defined shape in the material.

The XPS results also demonstrated in Fig. 5, with binding energies of elements expressed in eV. A peak at 284 nm arises due to the elemental carbon (Fig. 5a) [48,49], whereas Fig. 5b represents the oxygen 1s core level and main peak at 529 nm showed oxygen in Ti-O of titania network. The peaks at 457 and 454 nm representing titanium 2p core level (Fig. 5c).

Photocatalytic activity: The efficiency of calcined GT2 nanocomposite and pure TiO_2 as photocatalysts towards the photodegradation of methyl orange dye was evaluated in this study. The absorbance exhibited at different concentrations of MO and different dosage of calcined GT2 nanocomposite are illustrated in Table-1.

Volume of 10^{-5} M methyl orange (mL)	Absorbance	Amount of GT2 added to 10 mL 10^{-4} M methyl orange	Absorbance
2	0.16	0.02 g	0.18
4	0.22	0.03 g	0.14
6	0.27	0.04 g	0.13
8	0.32		
10	0.36		

Effect of amount: With increasing the calcined nanocomposite content, the photocatalytic activity was found to be enhanced as shown in Fig. 6. The percentage degradation efficiency of $\text{GT2}_{0.02}$ was 59% while $\text{GT2}_{0.03}$ and $\text{GT2}_{0.04}$ exhibited 71% and 75% degradation efficiency, respectively with day light irradiation of 45 min.

Effect of time: A study on degradation efficiency of $\text{GT2}_{0.03}$ at the time intervals of 15 min was also carried out. Table-2 shows that the degradation efficiency was found to be linearly increased with the irradiation time as there is chance for more and more photons to fall on the catalyst surface thereby creating increased amounts of photoexcited species causing degradation.

Comparative studies: Table-3 represents a comparison data of methyl orange dye degradation by various types of nanocomposites prepared by different methods. The graphene incorporated titania sample prepared by sonochemical route under

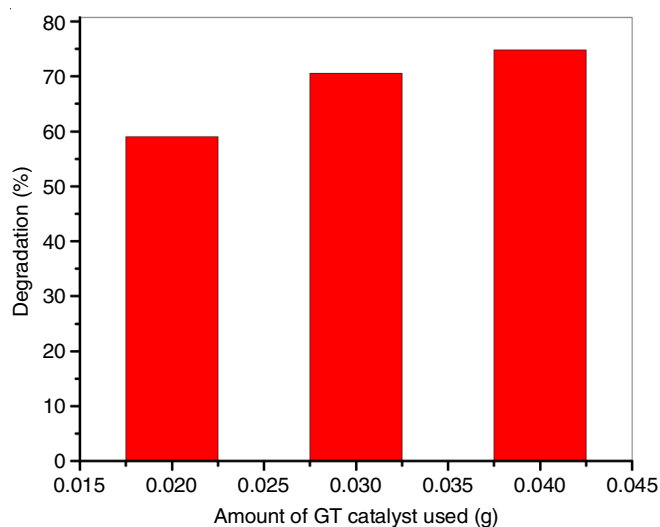


Fig. 6. Degradation graph showing percentage of degradation for varying amount of catalyst (GT2)

Time interval	Degradation (%)
After 15 min	53.1
After 30 min	62.8
After 45 min	70.6

UV light irradiation for 30 min showed 70% degradation efficiency, however, the calcined graphene-titania (GT2) nanocomposite showed higher degradation efficiency of 75% under sun light irradiation. Thus, due to the high surface area and high compatibility, calcined nanocomposite has better photocatalyst activity.

Conclusion

We successfully synthesized nanostructured graphene- TiO_2 nanocomposite by sonochemical method followed by calcination process at 400°C . The characterization results indicated that calcined nanocomposite has high surface area and high compatibility. By varying amount of the prepared nanocomposite, the photocatalytic efficiency can also be varied. About 75% photodegradation of methyl orange dye shows that the graphene-titania nanocomposite can degrade a target pollutant under certain conditions.

TABLE-3
COMPARISON DATA OF DEGRADATION OF METHYL ORANGE DYE USING
GRAPHENE INCORPORATED TITANIA PREPARED FROM DIFFERENT METHODS

Photocatalyst	Dye conc.	Catalyst conc.	Time (min)	Degradation (%)	Methods	Light source	Ref.
TGO	5 mg/L	100 mg	30	70	Sonochemical route	UV	[50]
TiO ₂	100 ppm	100 mg/L	60	14	Wet chemical method	Visible light	[51]
Co:La:TiO ₂	100 ppm	100 mg/L	60	45	Wet chemical method	Visible light	[51]
TiO ₂	20 mg/L	2.0 g/L	40	97.91	Degussa P25 from Degussa AG company in Germany	UV irradiation	[52]
TiO ₂ /ZnO heterojunction	20 mg/mL	0.1 g/L	30	97	Solvothermal method	UV light	[53]
Undoped CeO ₂	0.025 mM	–	120	15	Doctor blade method	Visible light	[54]
Fe-doped CeO ₂ 1.5% Fe doped in CeO ₂	0.025 mM	–	120	83	Doctor blade method	Visible light	[54]
TiO ₂	–	–	120	13.5	–	Visible light	[55]
Synthesized α-Fe ₂ O ₃ using glucose	20 mg/L	5 mg	100	82.17	Combustion process	UV lamp	[56]
Synthesized α-Fe ₂ O ₃ using sucrose	20 mg/L	10 mg	100	95.31	Combustion process	UV lamp	[56]
Ligand free CdS nano crystals	10 mg/L	10 mg	300	95	–	Visible	[57]
Graphene-TiO ₂ nanocomposite	0.1 mg/L	4 mg	45	74.8	Combined sonochemical and calcination method	Sunlight	Present study

CONFLICT OF INTEREST

The authors declare that there is no conflict of interests regarding the publication of this article.

REFERENCES

- N. Bhattacharjee, I. Som, R. Saha and S. Mondal, *Int. J. Environ. Anal. Chem.*, **104**, 489 (2022); <https://doi.org/10.1080/03067319.2021.2022130>
- J. Karpinska and U. Kotowska, *Water*, **11**, 2017 (2019); <https://doi.org/10.3390/w11102017>
- N. Morin-Crini, E. Lichtfouse, G. Liu, V. Balam, A.R.L. Ribeiro, Z. Lu, F. Stock, E. Carmona, M.R. Teixeira, L.A. Picos-Corrales, J.C. Moreno-Piraján, L. Giraldo, C. Li, A. Pandey, D. Hocquet, G. Torri and G. Crini, *Environ. Chem. Lett.*, **20**, 2311 (2022); <https://doi.org/10.1007/s10311-022-01447-4>
- M.T.H. Van Vliet, E.R. Jones, M. Florke, W.H.P. Franssen, N. Hanasaki, Y. Wada and J.R. Yearsley, *Environ. Res. Lett.*, **16**, 024020 (2021); <https://doi.org/10.1088/1748-9326/abbfc3>
- R. Li, T. Li and Q. Zhou, *Catalysts*, **8**, 804 (2020); <https://doi.org/10.3390/catal10070804>
- M.M. Mahlambi, C.J. Ngila and B.B. Mamba, *J. Nanomater.*, **2015**, 790173 (2015); <https://doi.org/10.1155/2015/790173>
- X. Kang, S. Liu, Z. Dai, Y. He, X. Song and Z. Tan, *Catalysts*, **9**, 191 (2019); <https://doi.org/10.3390/catal9020191>
- F. Tanos, A. Razzouk, G. Lesage, M. Cretin and M. Bechelany, *ChemSusChem*, **17**, e202301139 (2024); <https://doi.org/10.1002/cssc.202301139>
- A.K. Geim and K.S. Novoselov, *Nat. Mater.*, **6**, 183 (2007); <https://doi.org/10.1038/nmat1849>
- G. Eda, G. Fanchini and M. Chhowalla, *Nat. Nanotechnol.*, **3**, 270 (2008); <https://doi.org/10.1038/nnano.2008.83>
- J. Du, X. Lai, N. Yang, J. Zhai, D. Kisailus, F. Su, D. Wang and L. Jiang, *ACS Nano*, **5**, 590 (2011); <https://doi.org/10.1021/nn102767d>
- Z. Wang, M. Zhang, Z. Song, M. Yaseen, Z. Huang, A. Wang, Z. Guisheng and S. Shao, *J. Colloid Interface Sci.*, **624**, 88 (2022); <https://doi.org/10.1016/j.jcis.2022.05.094>
- S. Linley, Y.Y. Liu, C.J. Ptacek, D.W. Blowes and F.X. Gu, *ACS Appl. Mater. Interfaces*, **6**, 4658 (2014); <https://doi.org/10.1021/am4039272>
- S. Stankovich, D.A. Dikin, R.D. Piner, K.A. Kohlhaas, A. Kleinhammes, Y. Jia, Y. Wu, S.T. Nguyen and R.S. Ruoff, *Carbon*, **45**, 1558 (2007); <https://doi.org/10.1016/j.carbon.2007.02.034>
- B.Y.S. Chang, N.M. Huang, M.N. An'am, A.R. Marlinda, Y. Norazriena, M.R. Muhamad, I. Harrison, H.N. Lim, C.H. Chia, *Int. J. Nanomed.*, **7**, 3379 (2012); <https://doi.org/10.2147/IJN.S28189>
- S. Khanna, P. Marathe, S. Paneliya, P. Vinchhi, R. Chaudhari and J. Vora, *Int. J. Hydrogen Energy*, **47**, 41698 (2022); <https://doi.org/10.1016/j.ijhydene.2022.02.050>
- P. Muthirulan, C.N. Devi and M.M. Sundaram, *Mater. Sci. Semicond.*, **25**, 219 (2014); <https://doi.org/10.1016/j.mssp.2013.11.036>
- D.N. Tafen, J. Wang, N.Q. Wu and J.P. Lewis, *Appl. Phys. Lett.*, **94**, 093101 (2009); <https://doi.org/10.1063/1.3093820>
- J. Wang, D.N. Tafen, J.P. Lewis, Z. Hong, A. Manivannan, M. Zhi, M. Li and N. Wu, *J. Am. Chem. Soc.*, **131**, 12290 (2009); <https://doi.org/10.1021/ja903781h>
- J.M. Herrmann, *Catal. Today*, **53**, 115 (1999); [https://doi.org/10.1016/S0920-5861\(99\)00107-8](https://doi.org/10.1016/S0920-5861(99)00107-8)
- R. Asahi, T. Morikawa, T. Ohwaki, K. Aoki and Y. Taga, *Science*, **293**, 269 (2001); <https://doi.org/10.1126/science.1061051>
- V. Stengl, S. Bakardjieva and N. Murafa, *Mater. Chem. Phys.*, **114**, 217 (2009); <https://doi.org/10.1016/j.matchemphys.2008.09.025>
- N.R. Khalid, E. Ahmed, Z. Hong, L. Sana and M. Ahmed, *Curr. Appl. Phys.*, **13**, 659 (2013); <https://doi.org/10.1016/j.cap.2012.11.003>
- R. Nawaz, C.F. Kait, H.Y. Chia, M.H. Isa and L.W. Hwei, *Environ. Technol. Innov.*, **19**, 101007 (2020); <https://doi.org/10.1016/j.eti.2020.101007>
- J.P. Jeon, D.H. Kweon, B.J. Jang, M.J. Ju and J.B. Baek, *Adv. Sustain. Syst.*, **4**, 2000197 (2020); <https://doi.org/10.1002/adsu.202000197>
- L. Li, L. Yu, Z. Lin and G. Yang, *ACS Appl. Mater. Interfaces*, **8**, 8536 (2016); <https://doi.org/10.1021/acsami.6b00966>
- Y. Wang, L. Li, H. Lu, C. Wang, Y. Zhao, S. Kuga, Y. Huang and M. Wu, *J. Phys. Chem. Solids*, **162**, 110448 (2022); <https://doi.org/10.1016/j.jpcs.2021.110448>
- N. Ahmed, A.A. Farghali, W.M.A. El Roubay and N.K. Allam, *Int. J. Hydrogen Energy*, **42**, 29131 (2017); <https://doi.org/10.1016/j.ijhydene.2017.10.014>
- F. Li, Y. Huang, H. Peng, Y. Cao and Y. Niu, *Int. J. Photoenergy*, **2020**, 3617312 (2020); <https://doi.org/10.1155/2020/3617312>
- R. Kishor, D. Purchase, G.D. Saratale, L.F. Romanholo-Ferreira, C.M. Hussain, S.I. Mulla and R.N. Bharagava, *J. Water Process Eng.*, **43**, 102300 (2021); <https://doi.org/10.1016/j.jwpe.2021.102300>

31. X. Liu, Y. Yang, H. Li, Z. Yang and Y. Fang, *Chem. Eng. J.*, **408**, 127259 (2021); <https://doi.org/10.1016/j.cej.2020.127259>
32. Y. Yu, J.C. Yu, C.Y. Chan, Y.K. Che, J.C. Zhao, L. Ding, W.K. Ge and P.K. Wong, *Appl. Catal. B*, **61**, 1 (2005); <https://doi.org/10.1016/j.apcatb.2005.03.008>
33. S. Kohtani, S. Makino, K. Tokumura, Y. Ishigaki, T. Matsunaga, A. Kudo, O. Nikaido, K. Hayakawa and R. Nakagaki, *Chem. Lett.*, **31**, 660 (2002); <https://doi.org/10.1246/cl.2002.660>
34. S. Novoselov, A.K. Geim, S.V. Morozov, D. Jiang, Y. Zhang, S.V. Dubonos, I.V. Grigorieva and A.A. Firsov, *Science*, **306**, 666 (2004); <https://doi.org/10.1126/science.1102896>
35. M.Q. Yang, N. Zhang and Y.J. Xu, *ACS Appl. Mater. Interfaces*, **5**, 1156 (2013); <https://doi.org/10.1021/am3029798>
36. X.-Y. Zhang, H.-P. Li, X.-L. Cui and Y. Lin, *J. Mater. Chem.*, **20**, 2801 (2010); <https://doi.org/10.1039/b917240h>
37. S. Ali, A. Razaq and S. In, *Catal. Today*, **335**, 39 (2019); <https://doi.org/10.1016/j.cattod.2018.12.003>
38. M. Keshmiri, M. Mohseni and T. Troczynski, *Appl. Catal. B*, **53**, 209 (2004); <https://doi.org/10.1016/j.apcatb.2004.05.016>
39. W.S. Hummers Jr. and R.E. Offeman, *J. Am. Chem. Soc.*, **80**, 1339 (1958); <https://doi.org/10.1021/ja01539a017>
40. J.Y. Jang, M.S. Kim, H.M. Jeong and C.M. Shin, *Compos. Sci. Technol.*, **69**, 186 (2009); <https://doi.org/10.1016/j.compscitech.2008.09.039>
41. G. Jiang, X. Zheng, Y. Wang, T. Li and X. Sun, *Powder Technol.*, **207**, 465 (2011); <https://doi.org/10.1016/j.powtec.2010.11.029>
42. T.D. Nguyen-Phan, V.H. Pham, E.W. Shin, H.D. Pham, S. Kim, J.S. Chung, E.J. Kim and S.H. Hur, *Chem. Eng. J.*, **170**, 226 (2011); <https://doi.org/10.1016/j.cej.2011.03.060>
43. W. Fan, Q. Lai, Q. Zhang and Y. Wang, *J. Phys. Chem. C*, **115**, 10694 (2011); <https://doi.org/10.1021/jp2008804>
44. Y. Zhang, Z.R. Tang, X. Fu and Y.J. Xu, *ACS Nano*, **5**, 7426 (2011); <https://doi.org/10.1021/nn202519j>
45. D.C. Marcano, D.V. Kosynkin, J.M. Berlin, A. Sinitskii, A. Slesarev, Z. Sun, L.B. Alemany, W. Lu and J.M. Tour, *ACS Nano*, **4**, 4806 (2010); <https://doi.org/10.1021/nn1006368>
46. G. Jiang, Z. Lin, C. Chen, L. Zhu, Q. Chang, N. Wang, W. Wei and H. Tang, *Carbon*, **49**, 2693 (2011); <https://doi.org/10.1016/j.carbon.2011.02.059>
47. S. Sakhthivel and H. Kisch, *Angew. Chem. Int. Ed.*, **42**, 4908 (2003); <https://doi.org/10.1002/anie.200351577>
48. X.G. Gao, L.X. Cheng, W.S. Jiang, X.K. Li and F. Xing, *Front Chem.*, **9**, 615164 (2021); <https://doi.org/10.3389/fchem.2021.615164>
49. N. Serpone, *J. Phys. Chem. B*, **110**, 24287 (2006); <https://doi.org/10.1021/jp065659r>
50. M.D. Purkayastha, S. Sil, N. Singh, G.K. Darbha, S. Bhattacharyya, P.P. Ray, A.I. Mallick and T.P. Majumder, *FlatChem*, **22**, 100180 (2020); <https://doi.org/10.1016/j.flatc.2020.100180>
51. K. Azad and P. Gajanan, *Chem. Sci. J.*, **8**, 1000164 (2017); <https://doi.org/10.4172/2150-3494.1000164>
52. P. Niu, *Asian J. Chem.*, **25**, 1103 (2013); <https://doi.org/10.14233/ajchem.2013.13539>
53. R. Zha, R. Nadimicherla and X. Guo, *J. Mater. Chem. A Mater. Energy Sustain.*, **3**, 6565 (2015); <https://doi.org/10.1039/C5TA00764J>
54. D. Channei, B. Inceesungvorn, N. Wetchakun, S. Ukritnukun, J. Chen, A. Nattestad and S. Phanichphant, *Sci. Rep.*, **4**, 5757 (2014); <https://doi.org/10.1038/srep05757>
55. R. Raliya, C. Avery, S. Chakrabarti and P. Biswas, *Appl. Nanosci.*, **7**, 253 (2017); <https://doi.org/10.1007/s13204-017-0565-z>
56. R.K. Shah, *Arab. J. Chem.*, **16**, 104444 (2023); <https://doi.org/10.1016/j.arabjc.2022.104444>
57. P.C. Dey and R. Das, *Spectrochim. Acta A Mol. Biomol. Spectrosc.*, **231**, 118122 (2020); <https://doi.org/10.1016/j.saa.2020.118122>